

Improving organic transistor performance with Schottky contacts

Raoul Schroeder,^{a)} Leszek A. Majewski, and Martin Grell

Department of Physics & Astronomy, University of Sheffield, Hounsfield Road, Sheffield S3 7RH, United Kingdom

(Received 16 September 2003; accepted 8 December 2003)

Organic field-effect transistors (OFETs) with non-Ohmic contacts, e.g., pentacene with gold electrodes, exhibit a linearly growing threshold voltage with increased film thickness due to tunnel injection [R. Schroeder *et al.*, Appl. Phys. Lett. **83**, 3201 (2003)]. In this letter, we demonstrate gold/pentacene OFETs with a low threshold voltage independent of pentacene thickness. By doping the pentacene in the contact area with FeCl₃ (iron-III-chloride), the metal-insulator-type tunneling barrier was changed to a metal-semiconductor Schottky barrier. Since the injection through a Schottky barrier depends on the potential and not on the electric field, the threshold voltage is no longer a function of the semiconductor thickness. Through selective doping of the area under the electrode, the channel remains undoped, and large on/off ratios are retained. © 2004 American Institute of Physics. [DOI: 10.1063/1.1645993]

During the past few years, organic field-effect transistor (OFET) performance has been improved drastically through focused research efforts.^{1–4} This has led to the development of OFETs for commercial applications, where low production costs and flexible devices are desired.^{5–7} Many OFETs currently developed use pentacene as the semiconductor and gold as the electrode metal.^{5–8} However, an energy barrier of 0.85 eV (Ref. 9) to 1 eV (Ref. 10) exists between gold and pentacene, which leads to a thickness-dependent variation of the threshold voltage for a top contact architecture.¹¹ The increased threshold voltage with thickness is theoretically predicted; the injection into undoped organic molecular films can be described similar to a metal/insulator barrier with the Fowler-Nordheim equation.¹² We calculated the upper limit of the dopant concentration in these pentacene devices to be $5 \times 10^{11} \text{ cm}^{-3}$ from the channel off current. Therefore, the thickness of a theoretical Schottky barrier exceeds the thickness of the device by orders of magnitude, and the assumption that the interface behaves like a metal/insulator junction is valid.

In this letter, we present OFETs using gold electrodes on pentacene that exhibit low threshold voltages independent of the pentacene thickness through contact-area-limited doping. For this purpose, we evaporated FeCl₃ (a known dopant for *p*-type organic semiconductors¹³) under vacuum through the same shadow mask used for the subsequent gold sublimation to avoid contamination of the channel. The OFET shown in Fig. 1 was produced in the following manner: ITO on glass was etched in HCl to limit the overlap between the gate electrode and the source drain electrodes, as manifested in Fig. 1. Poly-(vinyl alcohol) (PVA), purchased from Aldrich, was spin-cast on top from a high-purity deionized water solution to a thickness of 110 nm. PVA is an insulating organic polymer with a dielectric constant of $\epsilon \approx 5$. Poly-(vinyl phenol) (PVP), also purchased from Aldrich, was subsequently spin-cast from a 2-propanol solution to a thickness of about 90 nm. PVP has a dielectric constant of $\epsilon \approx 2.8$. The thick-

ness of the double-layer structure was 200 nm, with a “combined dielectric constant” of $\epsilon = 3.9$, in good agreement with the theoretically predicted value. The reason to cap a high ϵ polymer with a low ϵ polymer is that it has been shown to improve mobilities.¹⁴

Pentacene was thermally sublimed on top of PVP *in vacuo*, and placing different samples at different positions in the bloom varied the thickness of the pentacene deposited, as we have previously shown.¹¹ The final thickness was then characterized with a surface profilometric measurement and an absorption measurement, with good agreement. The thickness was only varied by a factor of 4 in this batch, to keep

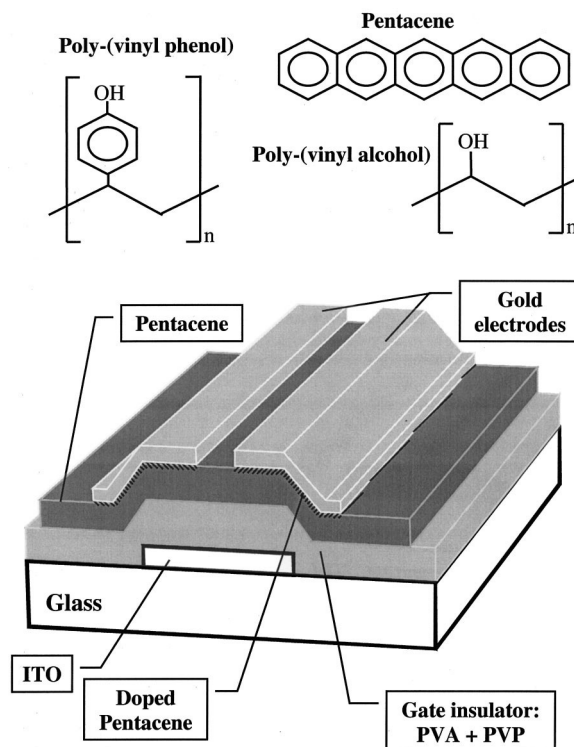


FIG. 1. Chemical structures of poly-(vinyl alcohol) (PVA), poly-(vinyl phenol) (PVP), and pentacene and the OFET device geometry investigated.

^{a)}Electronic mail: R.Schroeder@shef.ac.uk

TABLE I. Summary of the values for the threshold voltage and for the mobility for several devices with different thicknesses of the pentacene active semiconductor layer. The columns from left to right are as follows: t_{sc} is the semiconductor thickness, V_T is the threshold voltage (calculated from the linear fit of the field-effect current regime), and on/off ratio is the ratio of the source-drain current at $V_G = -5.5$ V over the source-drain current at $V_G = -0.5$ V.

t_{sc} (nm)	V_T (V)	μ [$\text{cm}^2(\text{Vs})^{-1}$]	On/off ratio
175	-1.55	2.6	1×10^3
250	-1.53	1.2	6×10^3
350	-1.45	1.2	5×10^3
400	-1.79	0.8	8×10^3

the deposition rate of pentacene near the optimum value of 5 Å/s for all samples. The pentacene thickness and the performance of all devices are recorded in Table I.

Finally, a very small amount of FeCl_3 (about 2×10^{-6} mg per contact area of 4 mm^2) and 60 nm of gold were evaporated through shadow masks that render the electrode areas as $2 \times 2 \text{ mm}^2$ with a distance of 40 microns (channel length). Therefore, pentacene is predominantly doped directly underneath the gold contacts, with little doping in the channel between the electrodes, which is of great importance for the transistor on/off ratio.¹³ We estimate from the amount of FeCl_3 deposited that the minimum doping-induced carrier concentration at the contacts is 10^{18} cm^{-3} . This indicates that the Schottky barrier width is a few nanometers at most.

These samples were characterized using two Keithley 2400 source-measure units, controlling the gate voltage and drain voltage, while measuring the gate leakage current and the drain current at the same time. The mobility and the threshold voltage were obtained by plotting the saturated drain current in the form of the square root of the drain current versus gate voltage (shown in Fig. 2). Mobility and threshold voltage were extracted from Fig. 2 with Eq. (1),

$$\sqrt{I_{D,\text{sat}}} = \sqrt{\frac{W}{2L} \frac{\mu \epsilon_0 \epsilon_i}{t_i}} (V_G - V_T), \quad (1)$$

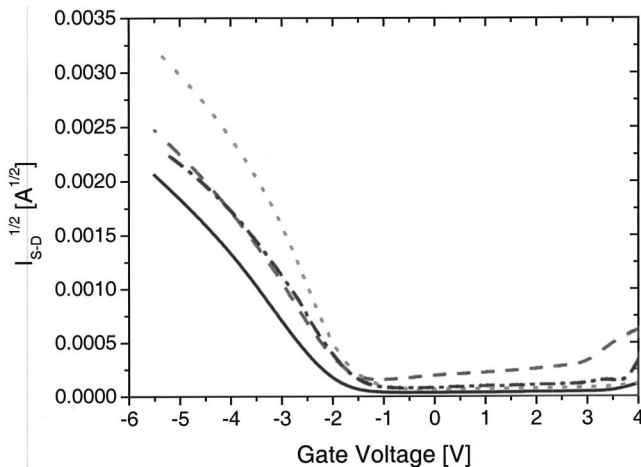


FIG. 2. OFET transfer characteristic, shown as the square root of the drain current vs gate voltage, while the drain voltage was held at -5 V. The solid curve depicts the 400-nm pentacene device, the dashed-dotted curve the 350-nm device, the dashed curve the 250-nm device, and the dotted curve the 175-nm device.

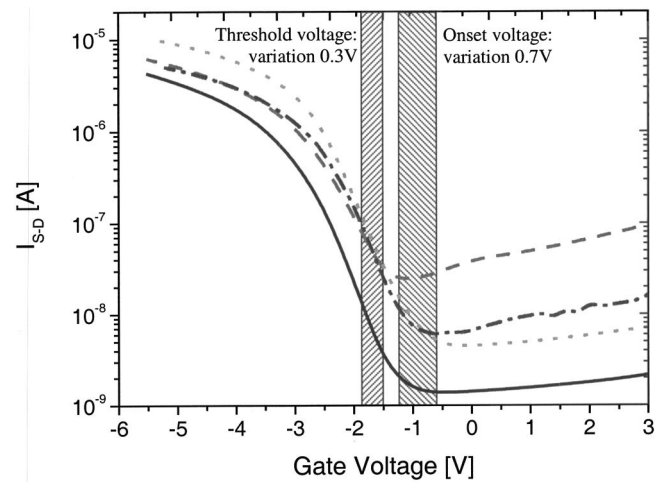


FIG. 3. Semilogarithmic plot of the OFET transfer characteristic with the drain voltage held at -5 V (data identical with Fig. 2). The line types for the different devices are identical to Fig. 2, i.e., solid, 400-nm device; dashed-dotted, 350-nm; dashed, 250 nm; dotted, 175 nm.

wherein $I_{D,\text{sat}}$ is the saturated drain current, V_G is the gate voltage, V_T is the threshold voltage, t_i is the thickness of the dielectric, L is the channel length, W is the channel width, and $\epsilon_0 \epsilon_i$ is the vacuum permittivity times the insulator dielectric constant.

In Fig. 2 it is seen that the current does not show a perfect quadratic behavior, but is lower than expected for higher gate voltages. In the literature, this effect has been attributed to gate stress¹⁵ and/or semiconductor stress¹⁶ (specifically for polymer OFETs) during the sweeps, increasing the threshold voltage. The threshold voltage for the contact-doped transistors, however, does not vary between measurements. In fact, in previous measurements on non-contact-doped transistors,¹¹ no deviation from the quadratic dependence occurred. Therefore, this effect is attributed to the contact doping with FeCl_3 . The explanation we offer is that the chlorine ions are not bound to the interface region and may drift during operation, slightly altering the transistor characteristic. This process, however, appears to be completely reversible. Still, the mobility of the dopands is a big issue, and will be addressed in the future.

Figure 3 depicts the semilogarithmic plot of the transfer characteristic shown in Fig. 2, visualizing the on/off ratios and subthreshold slopes. Threshold voltage, mobility, and on/off ratios are recorded in Table I. Equation (1) defines the threshold voltage as the point where the source-drain current starts to depend quadratically on the gate voltage; the assumption leading to Eq. (1) is that the transistor is perfectly off below the threshold voltage, as there is no accumulation layer. It is, however, well known that some transistor currents occur in the weak depletion regime, which is the regime near the onset voltage (the lowest absolute current in the transfer characteristic) and the threshold voltage. The onset voltage, which is better seen in Fig. 3 (identical data as in Fig. 2 in a different representation), varies more dramatically (0.7 V) than the threshold voltage (0.3 V), which is attributed to the variation of doping levels between the different OFETs.

The most important result is immediately seen from the second column in Table I. The threshold voltage is essen-

tially constant at $V_T \approx -1.5$ V, with a variation of 0.3 V at most when the thickness of the samples varies from 175 nm (375 nm including the gate insulator) to 400 nm (600 nm including the gate insulator). In otherwise identical OFETs without Schottky contacts, the threshold voltage would change by at least 0.8 V over the same range of thicknesses.¹¹

Looking at the on/off ratios and the off currents in Fig. 3, however, we see that some accidental doping of the channel occurs. The amount of FeCl₃ dopant is identical for all devices, yet the thickness of the pentacene layer is not. Combined with the fact that the chlorine dopants are not entirely bound to the electrode interface area, the unintentional doping of the semiconductor bulk and channel increases with decreasing pentacene thickness. This is the reason why the thinner layers have worse on/off ratios. For a given semiconductor thickness, however, the dopant amount is easily fine-tuned to yield optimum device performance. It is, however, important to point out that the OFETs presented here achieve an on/off ratio of almost 10⁴ at a gate voltage of only 5 V due to the low inverse subthreshold slope of 0.5 V/decade, which is quite an important step towards the fabrication of OFETs compatible with transistor–transistor logic (TTL) voltage levels.

From Table I it is apparent that the device with the thinnest pentacene layer shows the highest mobility, similarly to what we have reported previously.¹¹ Although part of the pentacene is now doped, the penetration depth of the iron-III-chloride is a few nanometers at most, and therefore the transistor channels are still buried under a thick layer of very pure, undoped pentacene. The simple linear relationship from Ref. 11, however, does not apply any longer, since the amount of doping and the penetration depth of the dopants cannot be controlled exactly; moreover, the effects of the doping are strongly influenced by the pentacene thickness in the device, as evidenced by the varying on/off ratios.

In conclusion, we present organic field-effect transistors based on pentacene with gold electrodes that display low

threshold voltage independent of pentacene thickness. The contacts between pentacene and gold are transformed from metal/insulator injection to metal/semiconductor Schottky barriers by doping with iron-III-chloride. Thus, the threshold voltage does not increase with overall device thickness. Through avoiding or minimizing doping of the channel, the on/off ratios remain high, and the overall device performance is very good even at driving voltages of 5 V, important for future applications using TTL voltage levels. Finally, we expect that this method of contact-area-limited doping will lead to the production of *n*-type organic transistors with air-stable metal electrodes.

The authors wish to thank the EPSRC for support under research grants Nos. GR/R88328/01 and GR/S02303/01.

¹S. Scheinert, G. Paasch, M. Schrödner, H.-K. Roth, S. Sensfuß, and Th. Doll, *J. Appl. Phys.* **92**, 330 (2002).

²M. D. Austin and S. Y. Chou, *Appl. Phys. Lett.* **81**, 4431 (2002).

³J. Fraxedas, *Adv. Mater. (Weinheim, Ger.)* **14**, 1603 (2002).

⁴A. Salleo, M. L. Chabinyc, M. S. Yang, and R. A. Street, *Appl. Phys. Lett.* **81**, 4383 (2002).

⁵H. Klauk, G. Schmid, W. Radlik, W. Weber, L. Zhou, C. D. Sheraw, J. A. Nichols, and T. N. Jackson, *Solid-State Electron* **47**, 297 (2002).

⁶P. F. Baude, D. A. Ender, M. A. Haase, T. W. Kelley, D. V. Muires, and S. D. Theiss, *Appl. Phys. Lett.* **82**, 3964 (2003).

⁷H. Klauk, M. Halik, U. Zschieschang, G. Schmid, W. Radlik, and W. Weber, *J. Appl. Phys.* **92**, 5259 (2002).

⁸See, e.g., Y. Iino, Y. Inoue, Y. Fujisaki, H. Fujikake, H. Sato, M. Kawakita, S. Tokito, and H. Kikuchi, *Jpn. J. Appl. Phys., Part 1* **42**, 299 (2003).

⁹N. Koch, J. Ghijsen, A. Elschner, R. L. Johnson, J.-J. Pireaux, J. Schwartz, and A. Kahn, *Appl. Phys. Lett.* **82**, 70 (2003).

¹⁰N. J. Watkins, L. Yan, and Y. Gao, *Appl. Phys. Lett.* **80**, 4384 (2002).

¹¹R. Schroeder, L. A. Majewski, and M. Grell, *Appl. Phys. Lett.* **83**, 3201 (2003).

¹²R. H. Fowler and L. Nordheim, *Proc. R. Soc. London, Ser. A* **119**, 683 (1928).

¹³A. R. Brown, D. B. de Leeuw, E. E. Havinga, and A. Pomp, *Synth. Met.* **68**, 65 (1994).

¹⁴J. Veres, S. D. Ogier, S. W. Leeming, D. C. Cupertino, and S. M. Khaffaf, *Adv. Func. Mater.* **13**, 199 (2003).

¹⁵D. Knipp, R. A. Street, A. Volkel, and J. Ho, *J. Appl. Phys.* **93**, 347 (2003).

¹⁶R. A. Street, A. Salleo, and M. L. Chabinyc, *Phys. Rev. B* **68**, 085316 (2003).